

---

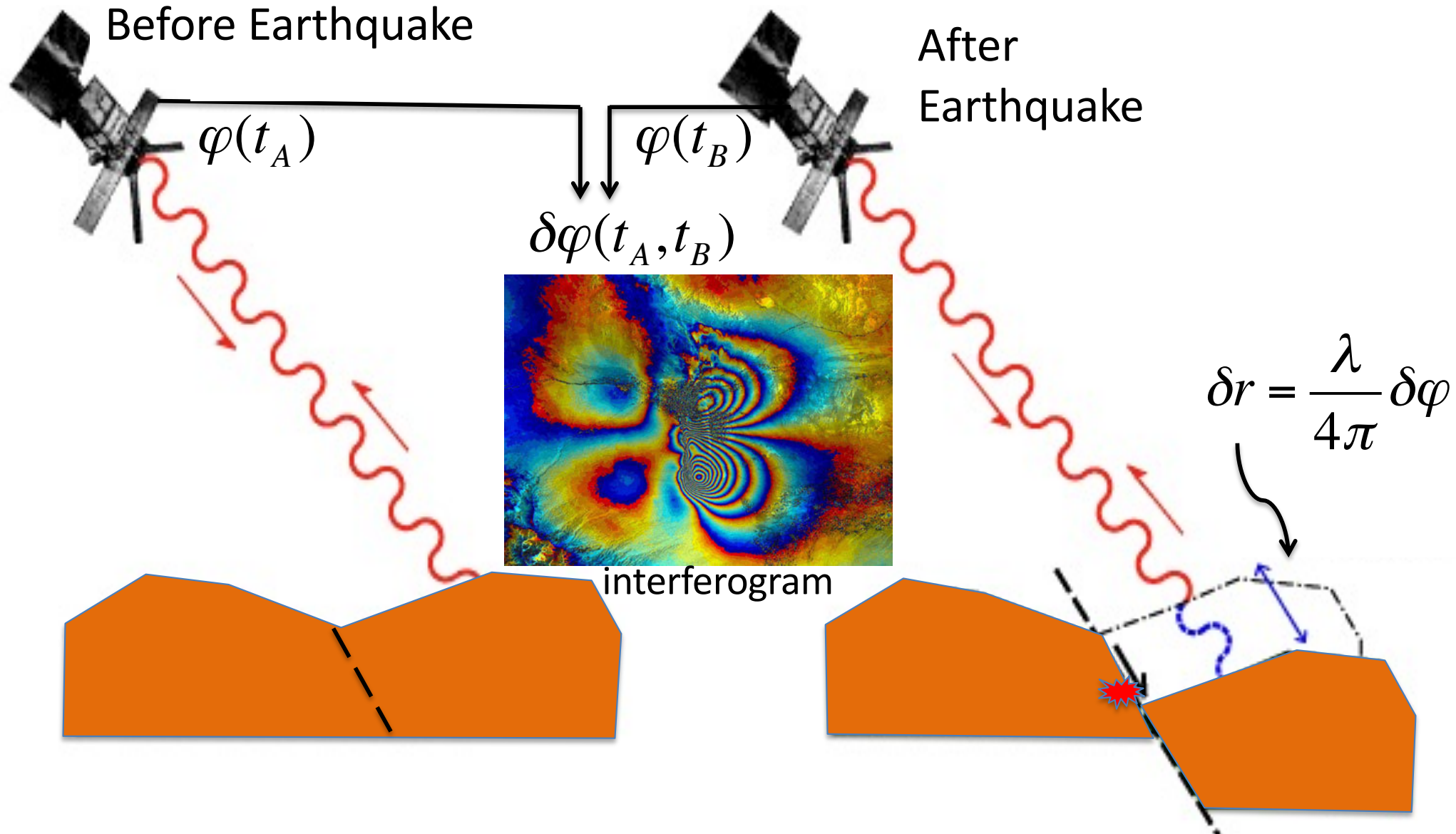
# Tropospheric delay in InSAR data

---

**Heresh Fattahi**

*(Jet Propulsion Laboratory, Caltech)*  
*Aug 2021*

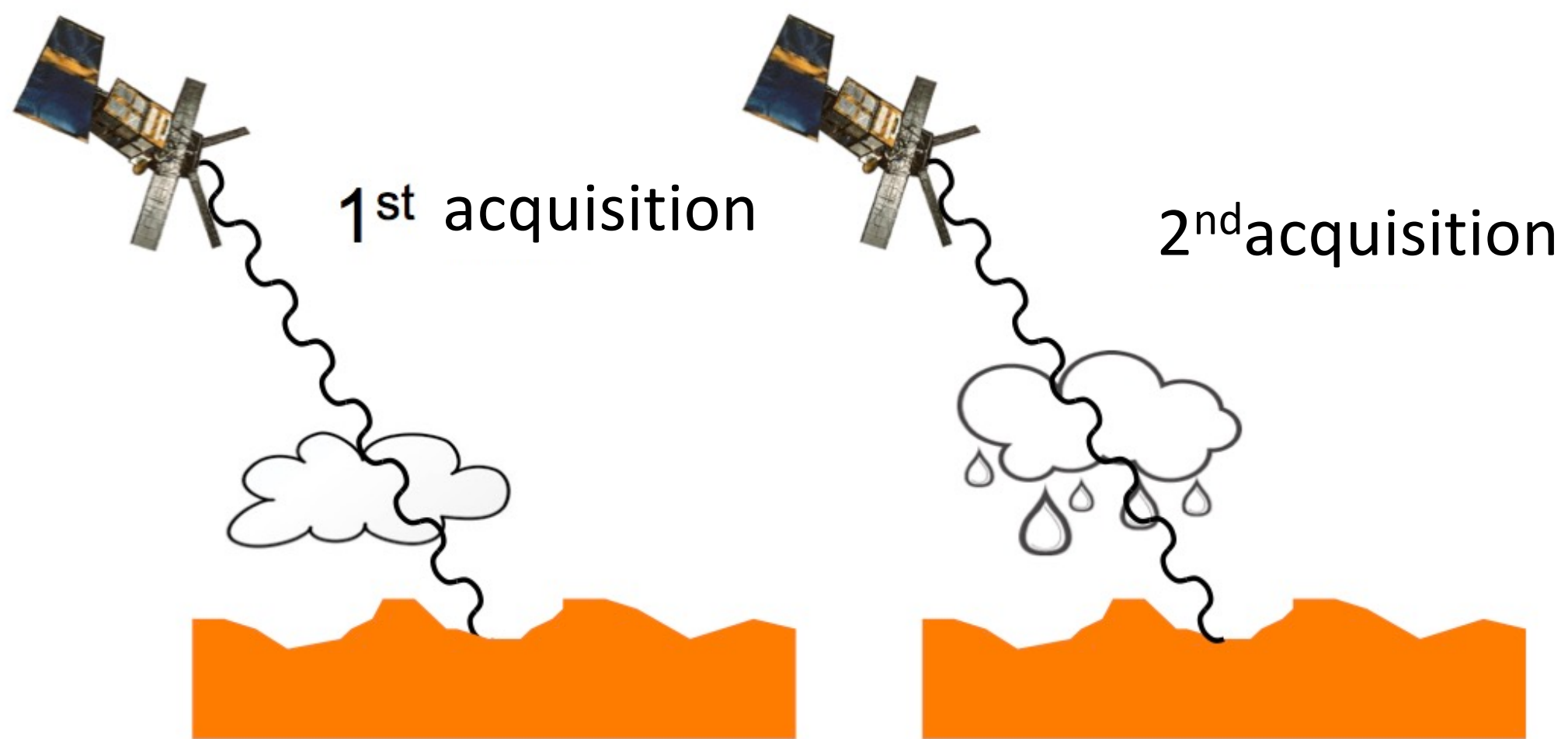
# InSAR (Interferometric Synthetic Aperture Radar )



$$\delta\varphi = \delta\varphi_{dis} + \delta\varphi_{atm} + \delta\varphi_{geometry} + \delta\varphi_{decor}$$

# Atmospheric delay

---



$$d = vt \quad v = \frac{c}{n}$$

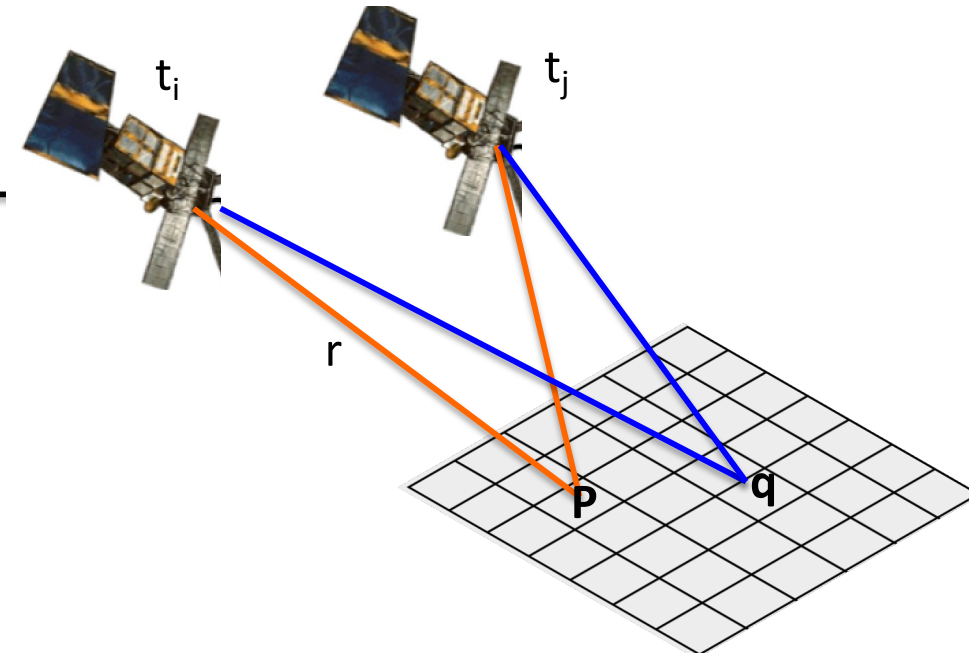
Index of refraction

$$\begin{cases} n = 1 & \text{vacuum} \\ n > 1 & \text{atmosphere} \end{cases}$$

[Modified from Z. Li]

## Atmospheric delay

Atmospheric delay for double difference InSAR measurements between two pixels ( $p$  and  $q$ ) and between acquisition times  $t_i$  and  $t_j$ :



$$\delta L_{pq}^{t_i, t_j} = \left[ \int_0^{r_p} N(r, t_j) dr - \int_0^{r_p} N(r, t_i) dr \right] - \left[ \int_0^{r_q} N(r, t_j) dr - \int_0^{r_q} N(r, t_i) dr \right]$$

With  $r$  the range from the radar to the target and  $N$  the refractivity

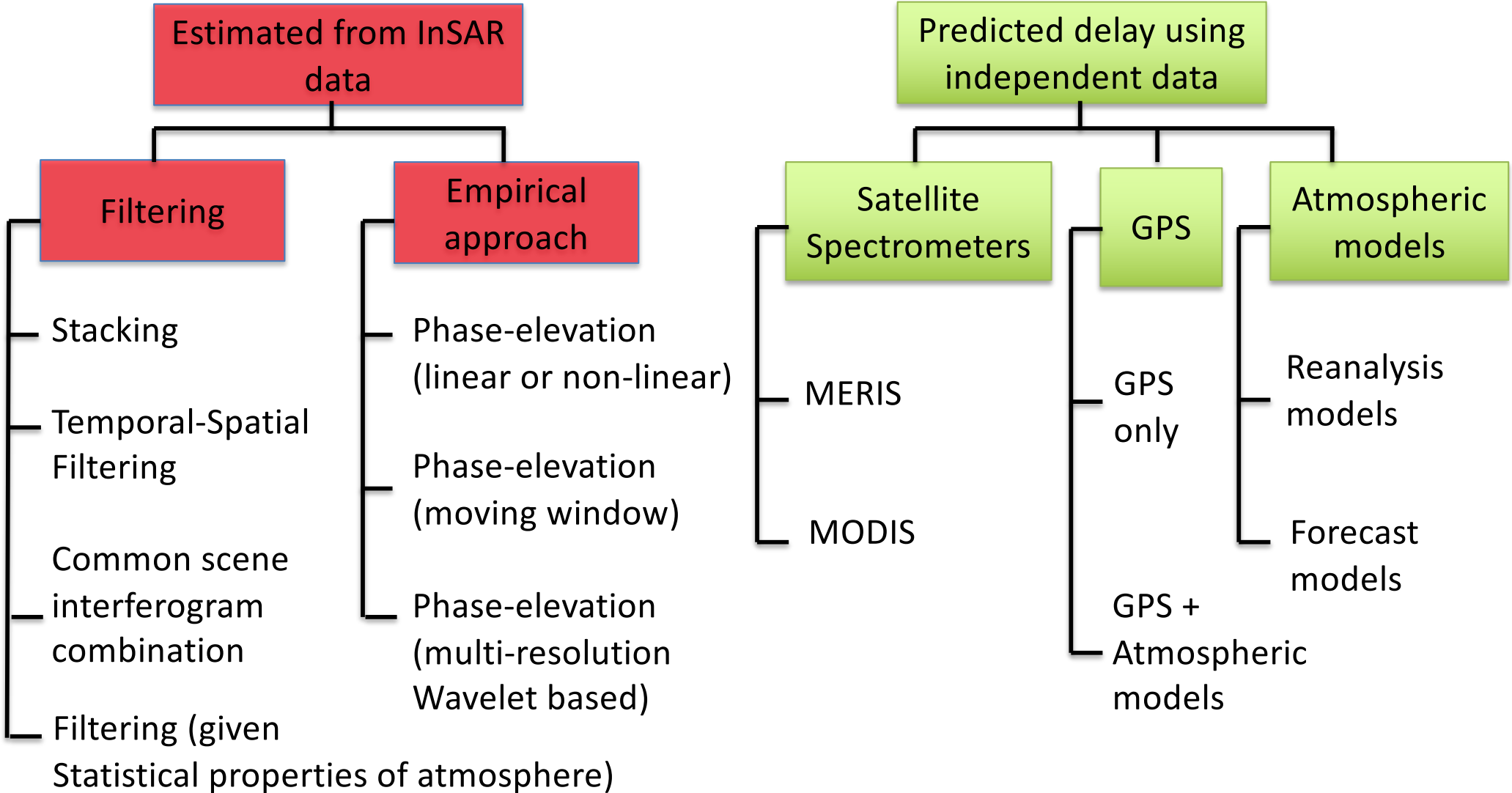
$$N = K_1 \frac{P_d}{T} + K_2 \frac{e}{T} + K_3 \frac{e}{T^2} + K_4 W_{cl} + K_5 \frac{ne}{f^2}$$

Troposphere      Cloud      Ionosphere

$P_d$ : dry air partial pressure,  $e$ : water vapor partial pressure,  $T$ : atmospheric temperature,  
 $W_{cl}$ : liquid water content [ $\text{kg}/\text{m}^3$ ],  $ne$ : electron number density/ $\text{m}^3$ ,  $f$ : radar frequency

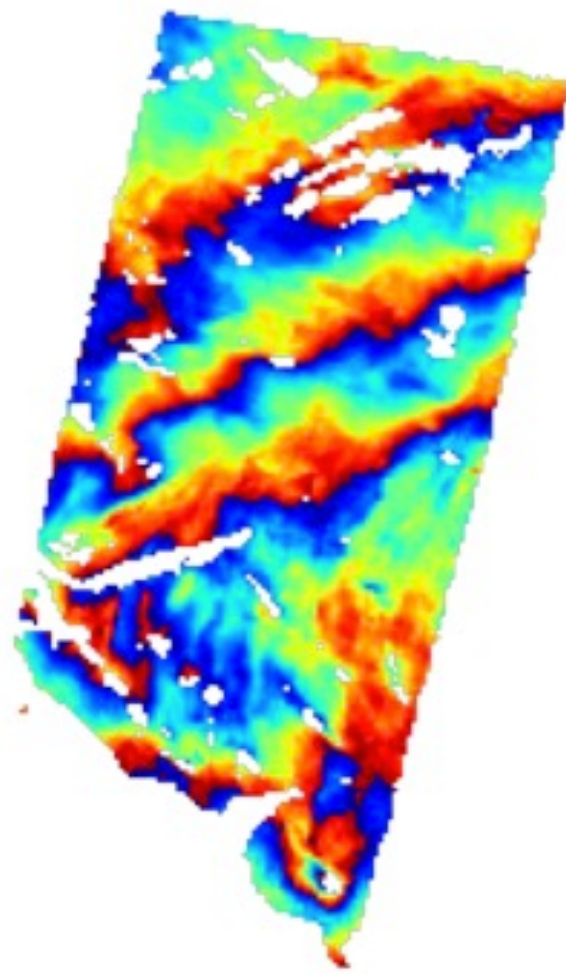
# Methods to correct the Tropospheric delay in InSAR data

---

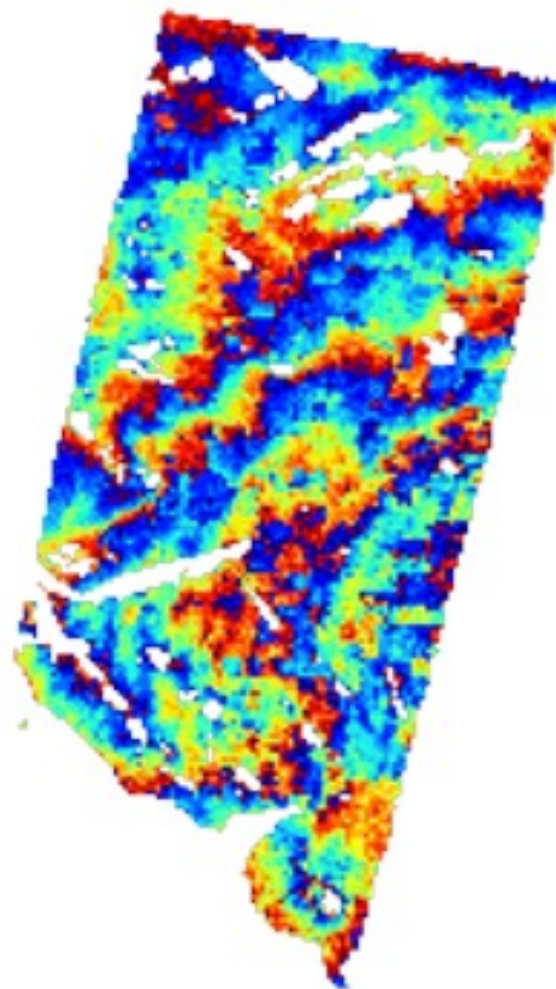


# Correction using MERIS

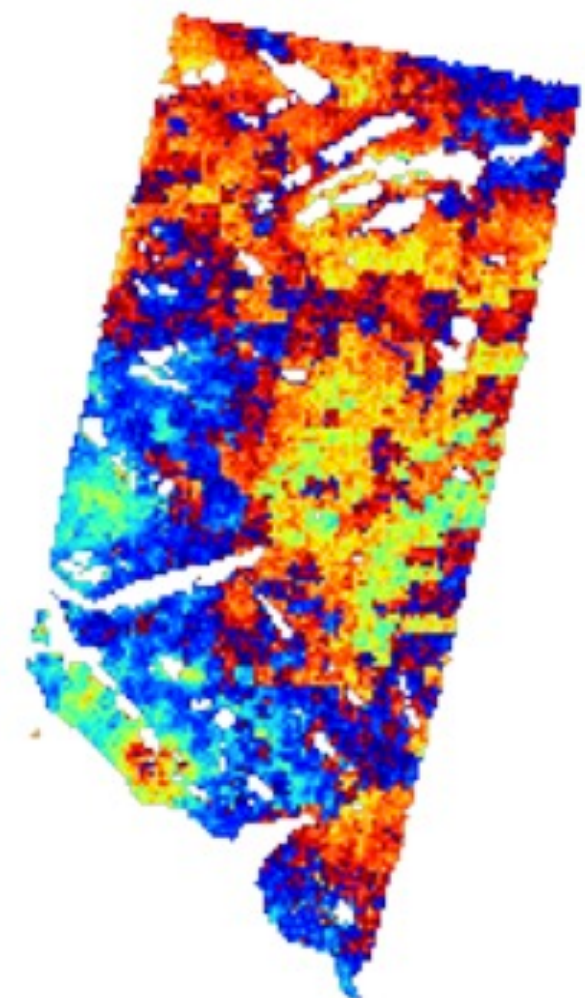
InSAR



MERIS (wet delay)



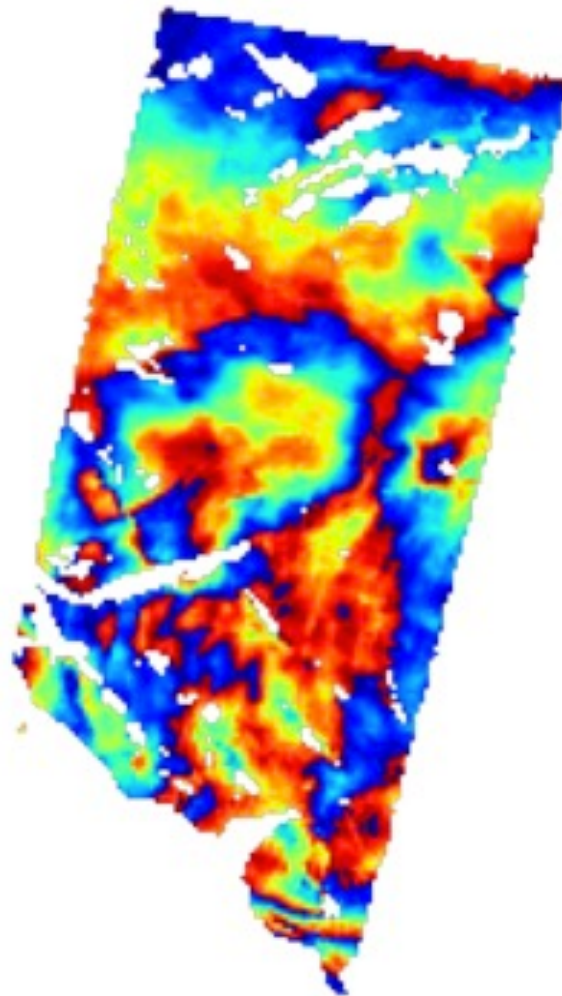
corrected InSAR



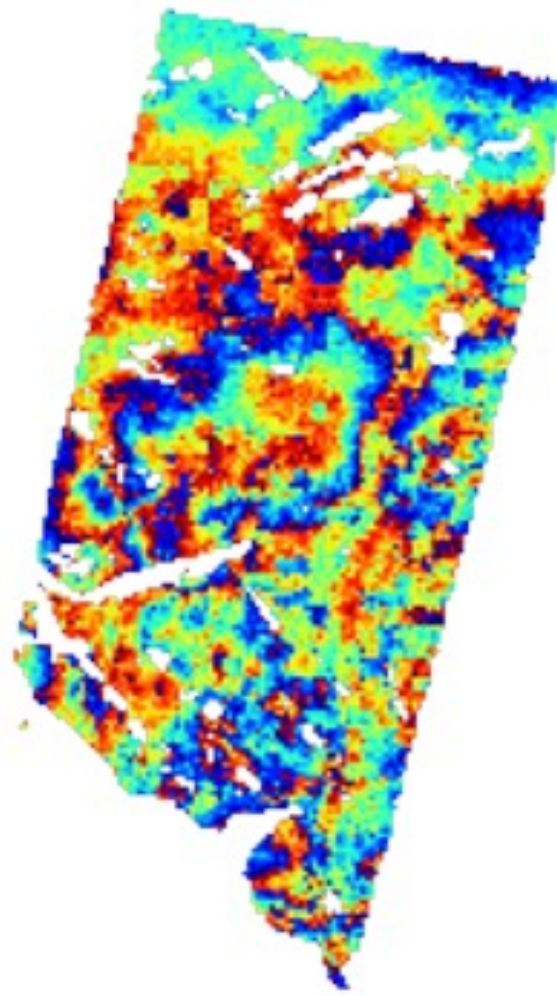
The interferogram is formed from ASAR data onboard Envisat which also was carrying a spectrometer called MERIS

# Correction using MERIS

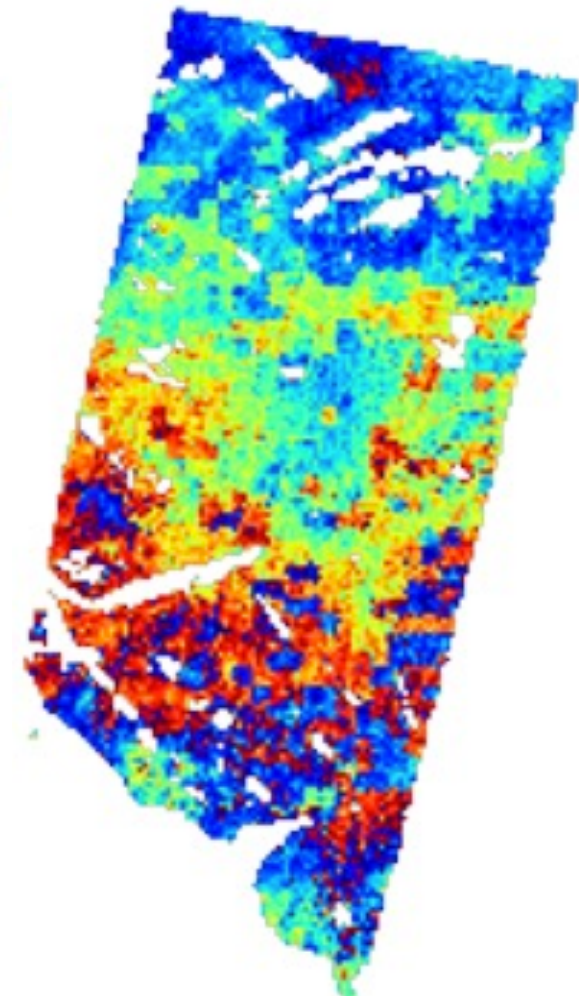
InSAR



MERIS (wet delay)



corrected InSAR



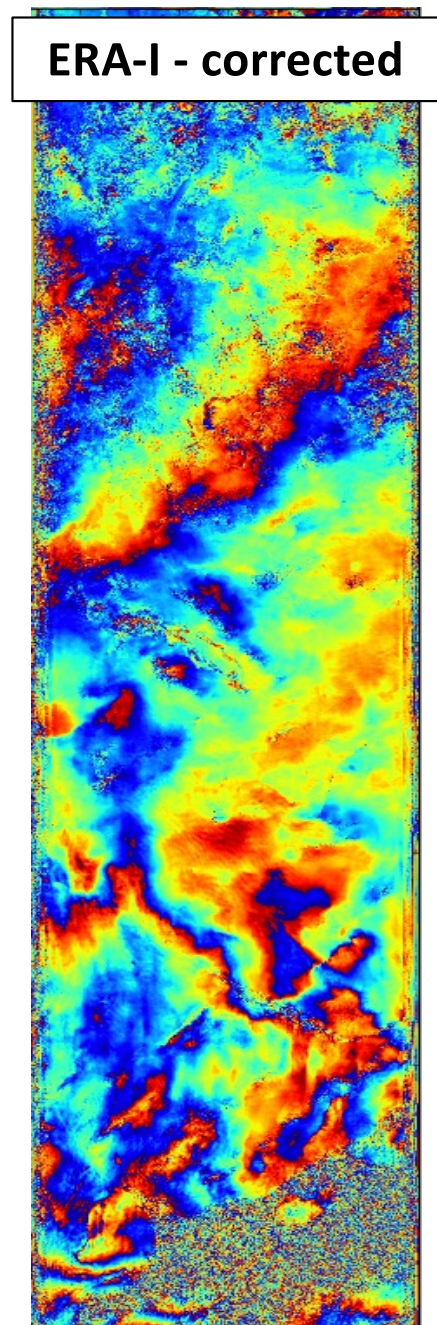
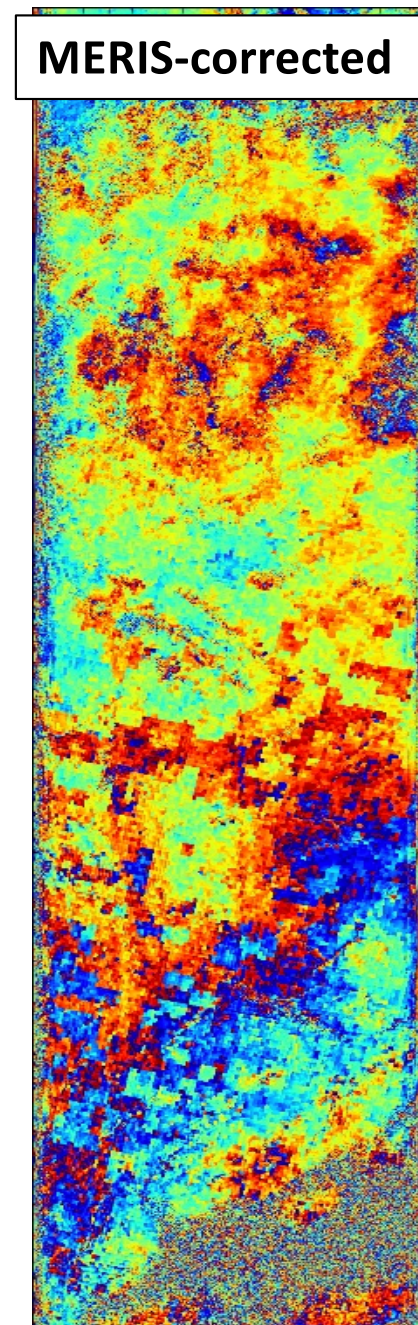
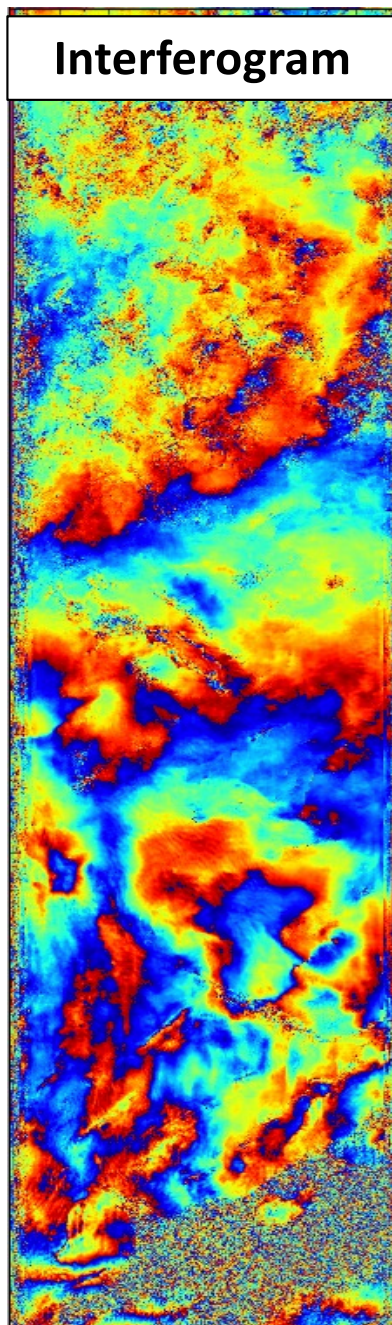
The interferogram is formed from ASAR data onboard Envisat satellite which also was carrying a spectrometer called MERIS

# Troposphere correction with MERIS and ERA-I

---

MERIS more accurate than atmospheric models.

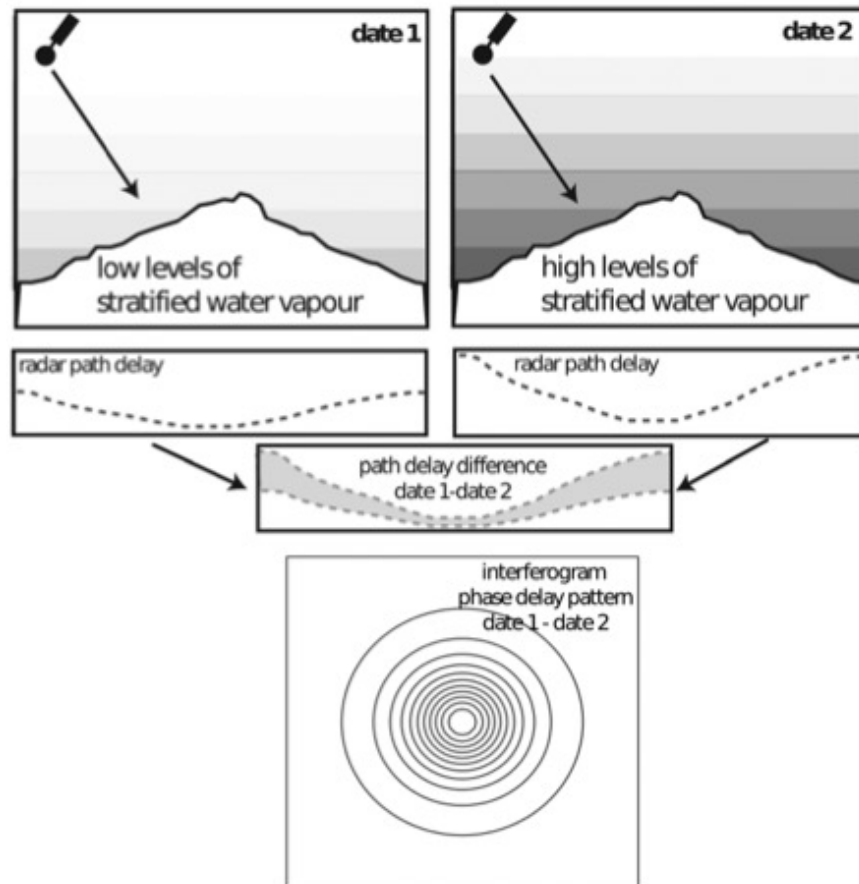
Limitations:  
Requires daylight,  
limited by cloud and  
not available at SAR  
acquisition time  
except for Envisat  
data.



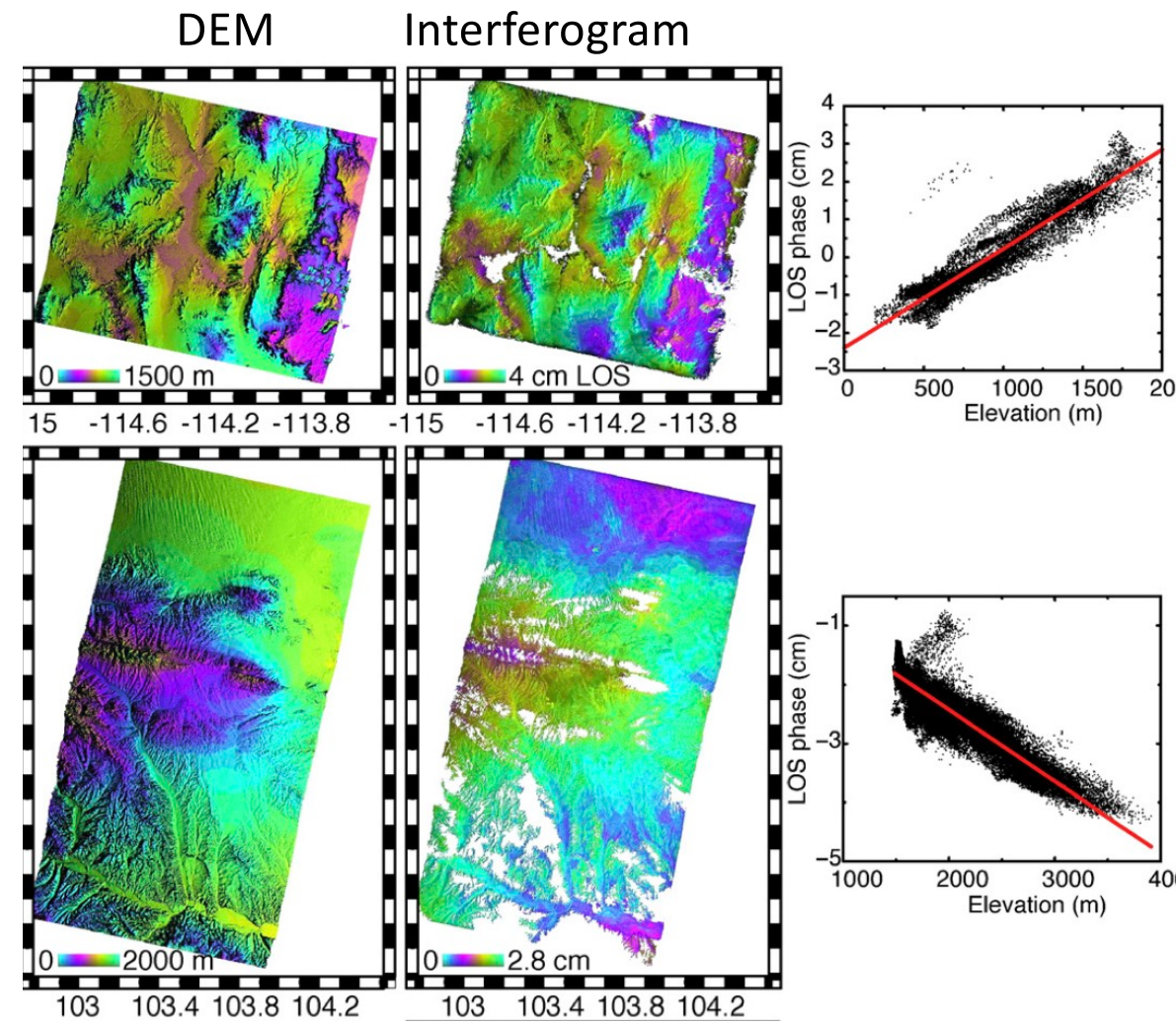
# Troposphere correction with Empirical approach

Caused by changes in tropospheric layering – correlates with topography (wet & dry)

Phase-elevation correlation can be estimated



Differences in tropospheric layering cause delays correlating with topography.



Empirical estimation across a portion or the whole scene

# Tropospheric delay correction with Atmospheric model (ERA-I)

Interferogram

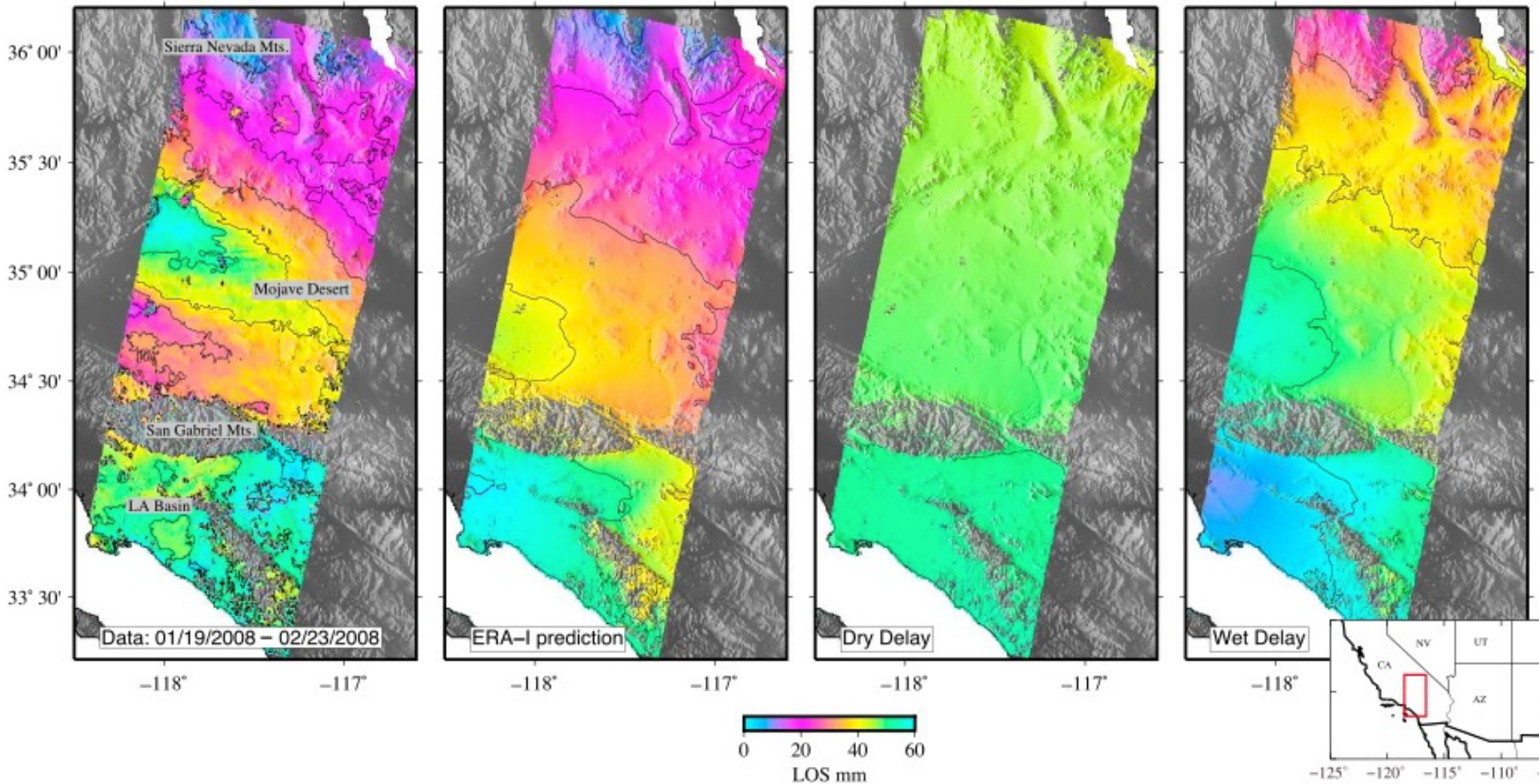
$$\Delta d_{tropo}$$

=

$$\Delta d_{dry}$$

+

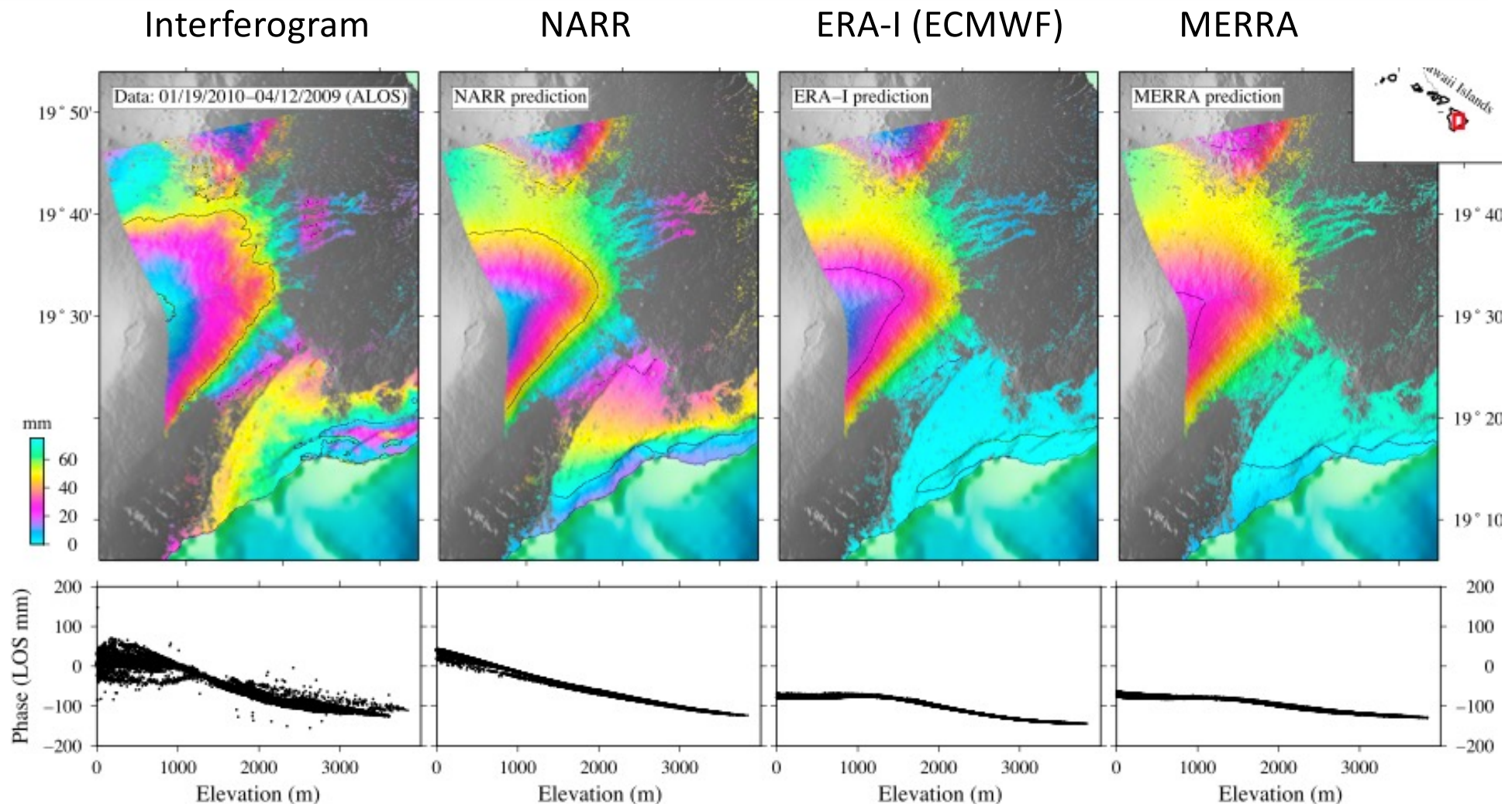
$$\Delta d_{wet}$$



$\Delta d_{dry} \ll \Delta d_{wet}$  as expected

[Jolivet et al, 2014]

# Troposphere correction with Atmospheric model (different models)



3 hours  
temporal  
spacing

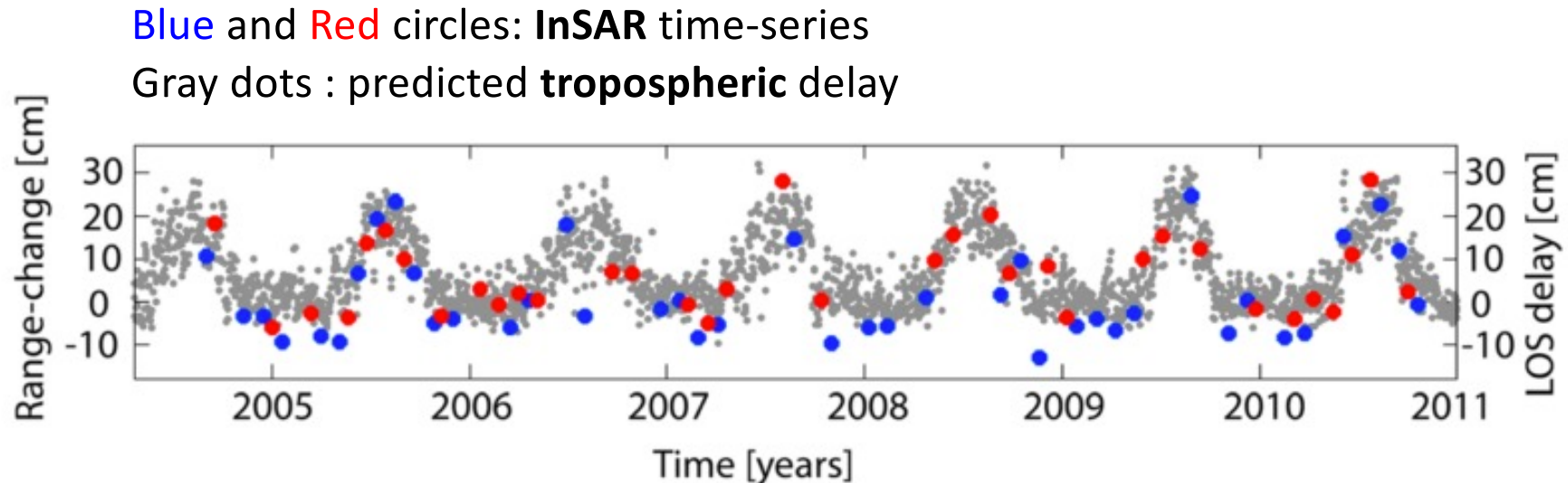
0.7° grid  
6 hours,  
37 levels

0.7° long, 0.5 lat  
6 hours  
42 levels

NARR performs best in this case

[Jolivet et al, 2014]

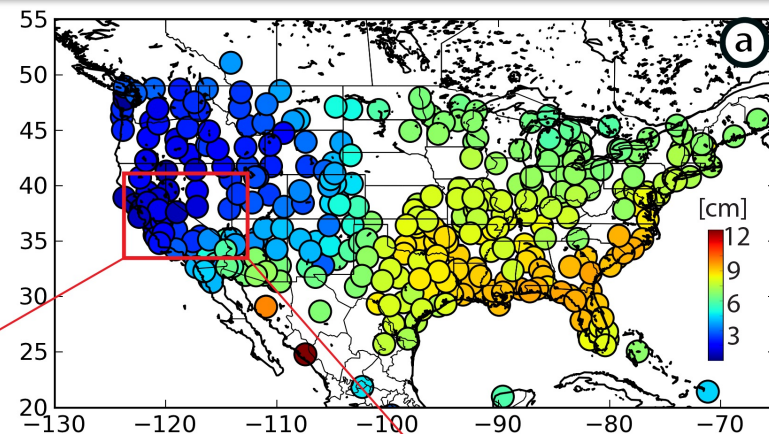
# Tropospheric delay has seasonal variations



The atmospheric models seem to successfully predict the seasonal delay while the improvement in the stochastic component may be minimal.

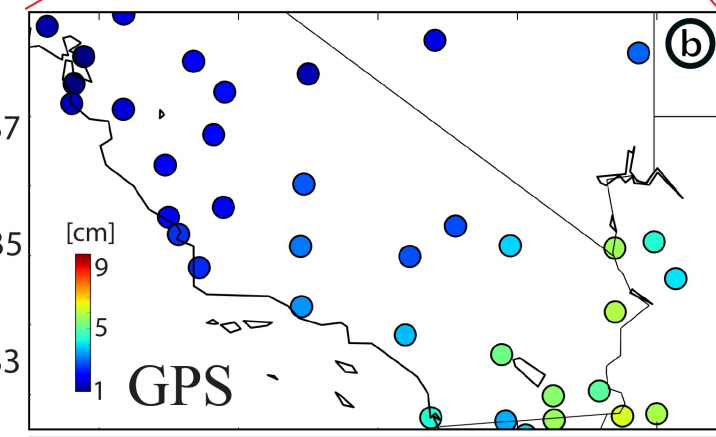
# Amplitude of the Seasonal delay across US

Smaller seasonal variation in western US

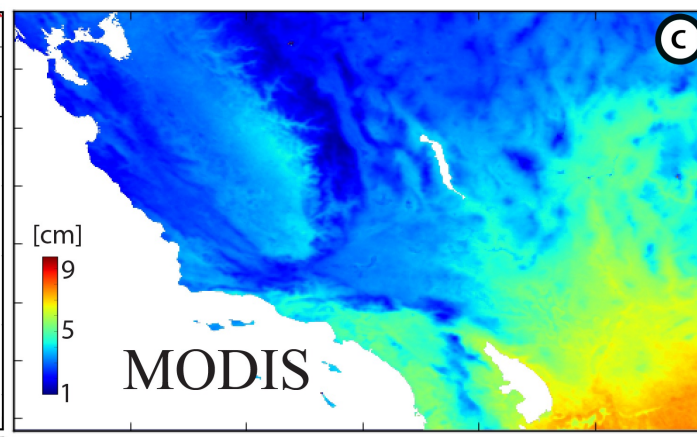


GPS, MODIS and ERA-I are consistent for the seasonal delay

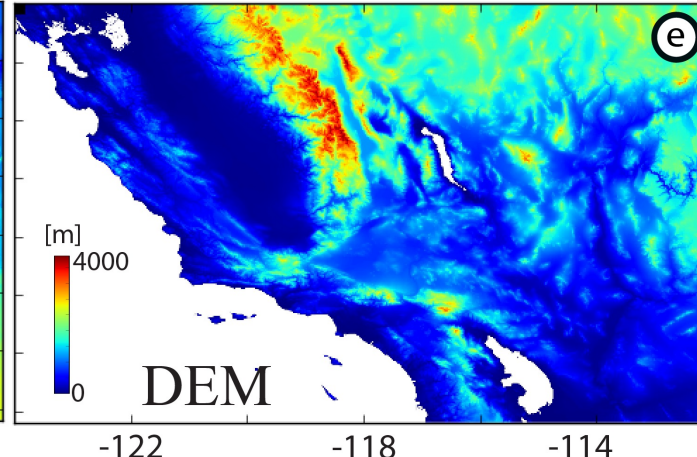
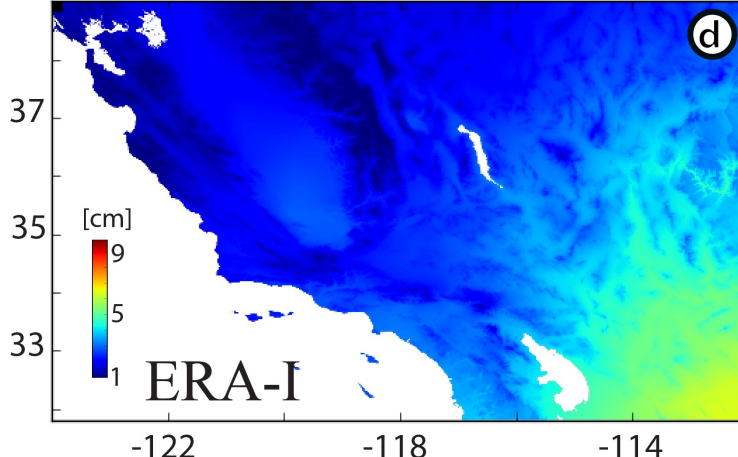
GPS delay  
(Unavco)

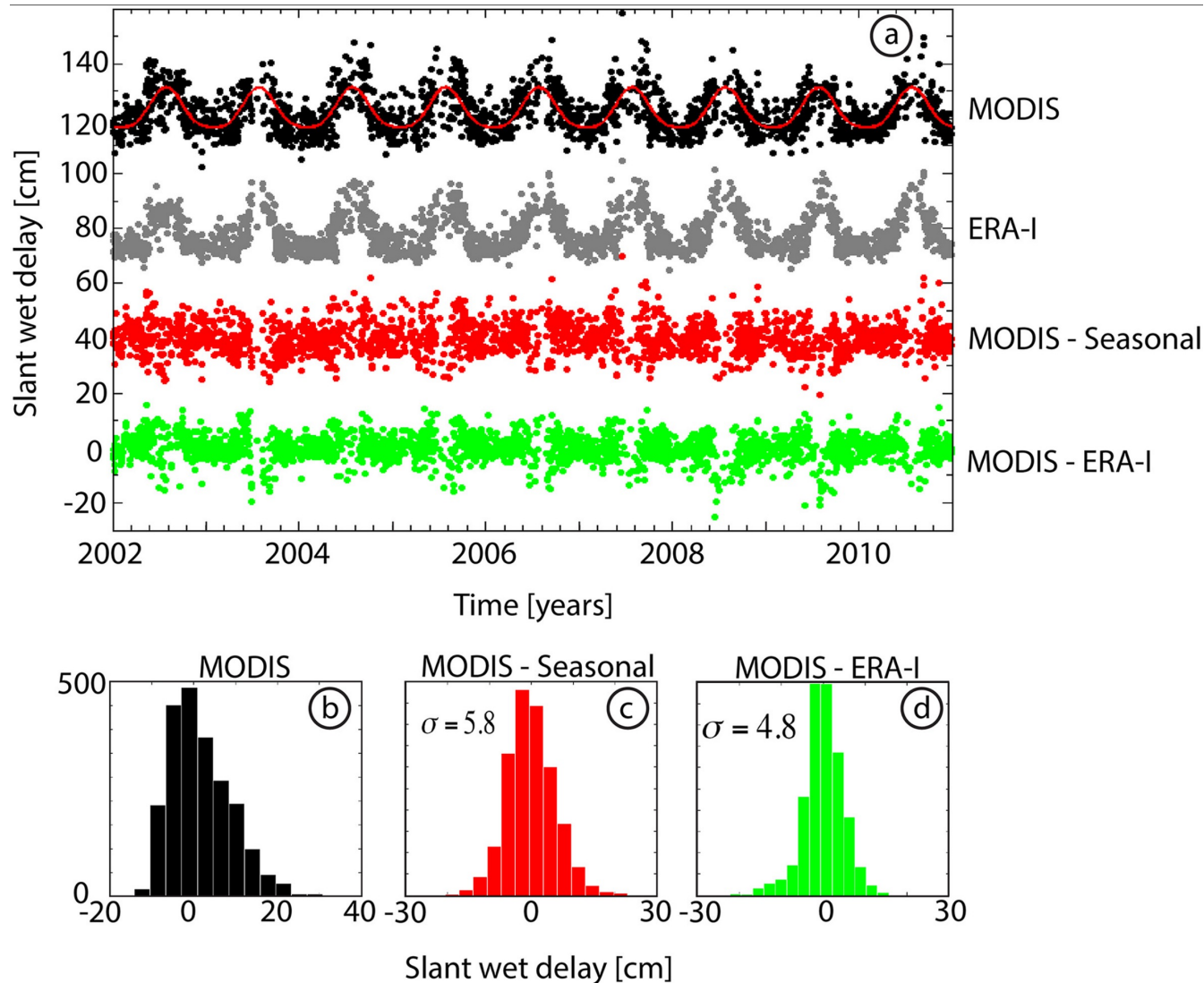


MODIS  
(NASA-JPL)



ERA-I  
(ECMWF and pyaps)





Tropospheric delay correction with atmospheric models accounts for systematic seasonal delay and reduces the standard deviation of the stochastic components by 10-20%.

## References:

Fattahi & Amelung, InSAR bias and uncertainty due to the systematic and stochastic tropospheric delay, JGR-Solid Earth, 2015.

<https://agupubs.onlinelibrary.wiley.com/doi/full/10.1002/2015JB012419>

Jolivet, R., P. S. Agram, N. Y. Lin, M. Simons, M. Doin, G. Peltzer, and Z. Li (2014), Improving InSAR geodesy using Global Atmospheric Models, *J. Geophys. Res. Solid Earth*, 119, 2324– 2341, doi:[10.1002/2013JB010588](https://doi.org/10.1002/2013JB010588).